Universität für Bodenkultur Wien
University of Natural Resources and Applied Life Sciences, Vienna
Department für Materialwissenschaften und Prozesstechnik
Department of Material Sciences and Process Engineering

Holztechnologie und Nachwachsende Rohstoffe
Wood Technology and Renewable Resources

Sabine Herzele

Wien, 10.12.2017

Marshall Plan Scholarship Scientific Report

Surface chemical properties of microfibrillated lignocellulose using inverse gas chromatography

Contract number: 742 926 21 17 2016

Table of content

Konrad Lorenz Straße 24, A-4330 Tulln an der Donau,
sabine.herzele@boku.ac.at

Sabine Herzele

Wien, 14.11.2017

Marshall Plan Scholarship Scientific Report

742 926 21 17 2016

Surface chemical properties of microfibrillated lignocellulose using inverse gas chromatography

To whom it may concern:

I finished my stay at the University of Maine, Advanced Structures and Composites Centre at September 24th. Herewith I send the final report of this stay.
The Marshall Plan Scholarship enabled me to make very good professional connection with the scientific staff of the working group of Prof. Douglas Gardner.
During the time spent abroad, I had the opportunity to get familiar with inverse gas chromatography (IGC), a technique for direct surface characterization for fibers and granular material. The characterized material was so-called microfibrillated cellulose (MFLC) obtained from wood pulp. Additionally, I was able to characterize the particle size of my specimens. I was not familiar with the fact that this device would be available at the Advanced Structures and Composites Centre. This was an appreciated surprise since the particle size is of great interest in combination with IGC measurements.
We (scientists from the Advanced Structures and Composites Center and BOKU) plan to publish the findings obtained during my stay in a joint publication. Please find in the following my detailed report of the IGC-measurements and the particle size measurements performed during my stay in the US. Since the preparation and characterization of the material was very time intense and complex I also add information about the preparation work for the material characterized in this report. In the section “additional information” I also added results obtained from morphology characterization of the material.

Best Regards

Sabine Herzele

Konrad Lorenz Straße 24, A-4330 Tulln an der Donau,
sabine.herzele@boku.ac.at

Abstract

M**icrofibrillated cellulose (MFC)** is usually produced by mechanical fibrillation of dilute aqueous suspensions of delignified wood pulp. From the fibrillation process typically fibrils with dimensions of 10-50 nm thickness and several µm lengths are obtained. As reinforcement agent in polymer composites, MFC has two major advantages compared to natural fibers: a) MFC is less prone to structural imperfections due to its small size and b) the large specific surface area of MFC offers a much higher potential for interfacial load transfer in polymeric matrices. The drawback of MFC as reinforcement agent is the **highly polar** surface which makes homogeneous dispersion in nonpolar solvents difficult. To overcome this challenge and establish compatibility between MFC and hydrophobic polymers, surface modification is required. Chemical surface modification is very efficient with regard to establishing compatibility between MFC and hydrophobic polymers, but it adds additional cost to MFC production.

It was repeatedly shown that high residual lignin- and hemicellulose content in MFC provides greatly improved miscibility with non-polar organic solvents or polymer melts, presumably due to the presence of non-polar moieties in lignin and moieties such as acetyl groups in hemicellulose. As a result, polymer composites reinforced with MFLC instead of MFC show improved mechanical performance compared to MFC-reinforced controls.

Strong evidence exists that surface-chemistry of MFLC differs significantly from MFC, and an amphiphilic character was proposed for MFLC.

The main purpose of my scientific visit at the University of Maine was to test the hypothesis that surface chemistry of MFLC differs significantly from MFC due to its residual lignin and hemicellulose content in the material by means of inverse gas chromatography (IGC).

Three spray dried (MFLC) powders obtained from beech wood with different lignin, hemicellulose and cellulose contents were characterized. As reference material, microfibrillated cellulose (MFC) isolated from straw was used. The reference material was virtually lignin free with only hemicellulose content lower than 10%

From IGC measurement characteristic dispersion surface energy (γ_s^d) on the solid surface of the powders can be obtained.

The results showed that the surface chemical properties of MFC can be tuned towards reduced hydrophilicity **with high residual lignin- and hemicellulose content of the microfibrillated cellulose.**

The findings propose that residual lignin and hemicellulose in MFLC instead of modification of MFC seem to be an interesting path worth following. Additionally, to the IGC-measurements, particle size analysis for all powders tested was performed.

Konrad Lorenz Straße 24, A-4330 Tulln an der Donau,
sabine.herzele@boku.ac.at

1. Frame and scientific outcome of visit

1.1 Justification of research visit

The University of Maine is a pioneering institution in the field of microfibrillated cellulose (MFC). The University of Maine Process Development Center (http://umaine.edu/pdc/facilities-available-for-use/nanocellulose-facility/) disposes of a pilot facility for nanocellulose production. Prof. Douglas J. Gardner is professor of Wood Science at the University of Maine. He is one of the key international experts in surface chemistry and adhesion issues of wood and cellulosic substrates as documented in numerous publications, e.g.[1],[2],[3] and inverse gas chromatography is one of the central techniques of his laboratory. Furthermore Prof. Gardner has a lot of experience with the application of different drying methods suitable for MFC (micro fibrillated cellulose) production. One major challenge in the MFC production is the conversion of MFC from the wet state into the dry state while preserving the structure as well as possible. The drying step is prerequisite for using MFC as a nanofiller in polymers. For this several drying techniques are available. In the last years Prof. Gardner`s working group conducted studies of different drying methods potentially suitable for CNC (cellulose nanocrystals) and NFC (nanofibrillated cellulose) production.[4] [5] [6] In a later work the impact of the different dying methods air drying, spray drying, super critical drying and freeze drying on the surface energy of cellulosic material were investigated by means of inverse gas chromatography.[7] Thus **Prof. Gardner combines expertise on MFC with expertise on inverse gas chromatography and different drying methods for cellulosic material** not available at BOKU. Since it is expected that applying this method to the characterization of lignin-containing MFC powders will provide a significant advance in the understanding of this interesting new type of MFC, a research visit to University of Maine is highly justified in view of the unique combination of expertise available with Prof. Gardner.

The results expected to arise from experiments to be carried out during the research visit at University of Maine will contribute an important part of my currently on-going doctoral studies. Through the establishment of collaboration with Prof Gardner, my work will benefit substantially in terms of developing a better understanding of the materials. On the mid-term, we expect in our group that the planned visit will initiate more regular exchanges between the groups of Prof. Gardner (University of Maine) and Prof. Gindl-Altmutter (BOKU).

1.2 Motivation

Declining fossil resources and growing concern about CO_2 emissions are important driving forces for research on bio-based materials. Cellulose, the most abundant biogenic materials, have been used by mankind since its beginnings, for construction, textiles, ropes, and many more. Currently, wood industry and the pulp and paper sector are important mass users of cellulosic resources and certainly will continue to be so in future. Recently, the use of cellulosic fibers for materials, e.g. aiming at substituting energy intensive glass fiber in polymer

reinforcement, has gained attention. Fibers from annual plants such as flax, hemp, jute, or kenaf are used in polymer reinforcement, but in terms of mechanical performance these fibers are clearly inferior to glass fiber. While carefully extracted individual fibers may dispose of comparably high strength and stiffness, current industrial fiber-isolation methods together with natural variability of fiber structure only deliver material of modest mechanical performance at high variability[8,9]. The discovery of **microfibrillated cellulose (MFC)**, which is usually produced by mechanical fibrillation of dilute aqueous suspensions of delignified wood pulp into typically 10-50 nm thick and several µm long fibrils, opened up an alternative path for cellulosic fiber utilization. MFC has two major advantages compared to natural fibers: a) MFC is less prone to structural imperfections due to its small size and b) the large specific surface area of MFC offers a much higher potential for interfacial load transfer in polymeric matrices or the generation of high internal surface in porous structures. These advantages contribute to the excellent mechanical performance of MFC-based composites comparable to- or even superior to those consisting of technical fibers, e.g. glass fiber [9,10,11]. Due to an abundance of accessible hydroxyl groups, **cellulose is essentially highly polar** in surface-chemical terms, even if a small fraction of the cellulose I crystal is classified hydrophobic [10]. Homogeneous dispersion in water and water-soluble polymers can therefore be easily achieved. By contrast, dispersion of cellulose in nonpolar solvents or polymers requires chemical modification[11]. Chemical surface modification is very efficient with regard to establishing compatibility between MFC and hydrophobic polymers, but it adds additional cost to MFC production, which is economically speaking - potentially critical with regard to high-volume applications of MFC in polymer reinforcement. Therefore, simple low-cost alternatives for establishing compatibility between hydrophobic media and MFC are highly desirable.

Since MFC is produced in aqueous condition, usually at only little percent solid content, the removal of water without loss of nano-scale morphology due to **collapse and hornification**, which happens during conventional drying, constitutes a critical processing step. Different sophisticated drying methods such as spray-drying, freeze drying, and supercritical drying were studied as potential alternatives to conventional drying [4]. While freeze drying and supercritical drying preserve fibrillary structures to a large extent, the dried product is highly networked, which may hinder re-dispersion. By contrast, spray drying yields individual particles of variable sizes, which may be well dispersed in polymers. Hornification may be circumvented by surface-chemical modification, e.g. carboxymethylation, prior to drying [12], which then enables re-dispersion. However, all these methods entail either additional cost, which may be substantial in the case of spray drying, freeze drying or supercritical drying, unsatisfying reinforcement efficiency, or need for chemical modification.

CNF-reinforced polymer nanocomposites are controlled mainly by: 1. agglomeration of cellulose fibers, 2. interaction between cellulose and polymer, 3 wetting of cellulose fibers and distribution and 4. dispersion of cellulose fibers within the polymer matrix. All these properties are directly related to surface energy of the cellulosic material.[7]

Konrad Lorenz Straße 24, A-4330 Tulln an der Donau,
sabine.herzele@boku.ac.at

A limited number of publications in literature [13], [14],[15] and recent own work [16], [17], [18], [19] indicate that **microfibrillated cellulose with high residual lignin- and hemicellulose content (MFLC)** may constitute an elegant way to circumvent several hurdles in the compounding of MFC with certain non-polar polymers. It was repeatedly shown that high residual lignin- and hemicellulose content in MFC provides greatly improved miscibility with non-polar organic solvents or polymer melts. The dispersion of MFC is greatly improved by the presence of lignin- or hemicellulose, presumably due to the presence of non-polar moieties in lignin and moieties such as acetyl groups in hemicellulose. As a result, polymer composites reinforced with MFLC instead of MFC show improved mechanical performance compared to MFC-reinforced controls. **Strong evidence exists that surface-chemistry of MFLC differs significantly from MFC, and an amphiphilic character was proposed for MFLC.**

1.3 Purpose of the visit

The main purpose of this scientific visit at the University of Maine was to test the hypothesis that surface chemistry of MFLC differs significantly from MFC due to its residual lignin and hemicellulose content in the material.

For the measurement of the spray-dried MFLC with different lignin and hemicellulose content, it was intended to use inverse gas chromatography (IGC), available at the University of Maine.

Inverse gas chromatography (IGC) is known to be the method of choice for this task, because it allows comprehensive characterization of small, granular or fibrous materials.

In particular, the acid-base components and the dispersive components of surface free energy can be determined.

Furthermore, the particle size of the powders was studied to obtain information about the morphology of the material.

1.4 Resulting publications

One publication will result out of the work performed at the Advanced Structures and Composites Center at the University of Maine.

The publication will deal with the surface chemical characterization by means of inverse gas chromatography (IGC) of spray dried $MFLC_{1-3}$ powders and MFC used as a reference material. Furthermore, the results from the particle size measurements of the material will be presented in this publication. Additionally, we plan to add information of the carbon and oxygen chemistry on the specimens. For this the surface sensitive x-ray photon spectroscopy measurement (XPS) will be applied. Furthermore, results of atomic force microscopy measurements (AFM) of MFLC fibrils and scanning probe microscopy (SEM) images of the spray dried specimens will be presented in this publication..

2. Production of the material

2.1 Organosolv treatment of the material

Microfibrillated lignocellulose (MFLC): Bark-free beech wood chips were partly delignified in a water/ethanol (50/50 weight) mixture (ethanol with purity of 96.6 % denatured with 1 % petroleum ether, Brüggemann Alkohol, Heilbronn, Germany) in batches of 6 kg (dry mass). At a mass ratio of 1:4 (wood/solvent), three different variants as shown in **Table 1** were processed in an autoclave. Sulfuric acid was added to catalyze delignification and enabling pulping at lower temperature. Based on the previous results a progressive lignin removal from variant $MFLC_2$ and $MFLC_3$ could be achieved by addition of 0.25 and 0.75 % sulfuric acid (95 %, Fischer Scientific, Schwerte, Germany) based on the dry weight of wood [20]

Table 1: *Treatment parameters for partial delignification in water/ethanol mixture*

Specimen type	Temperature [°C]	Pressure [bar]	H_2SO_4	Duration [min]
$MFLC_1$	170	15	0	90
$MFLC_2$	170	15	0.25	90
$MFLC_3$	170	15	0.75	90

Several studies indicate that sulfuric acid accelerates delignification in an organosolv process [21]. After the organosolv treatment, the reactor was cooled down to 40 °C and the material was washed with a 50/50 water/ethanol mixture to remove dissolved substances, in particular lignin. After three additional washing cycles in water the material was processed into fibers in a disc refiner. Excess water was removed by centrifugation and the material was refrigerated at -20 °C before further usage. [18]

Figure 1*: Wood chips before (left) and after organosolv treatment (right)*

Konrad Lorenz Straße 24, A-4330 Tulln an der Donau,
sabine.herzele@boku.ac.at

2.2 Mechanical disintegration of the material

After defrosting the fibrillated material was stored in a 3% deionized water suspension at room temperature to swell for 18 hours.

Grinding of the material was carried out with five passes through a Masuko Supermasscolloider (MKCA6-2J, Masuko Sangyo, Japan) at 1500 rotation per minute (corresponding to 25 Hz) and a nominal gap clearance of -50 lm. In this device, the fiber suspension is poured between two grinding stones, the upper one being fixed and the lower one rotating. The efficiency of the fibrillation is determined by the two previously described parameters, namely rotation rate and gap between the plates. Note that despite setting a negative nominal clearance a gap forms during operation of the grinder because of the hydrodynamic pressure of MFC slurry exiting from the space between the two rotating discs of the grinder.[18]

In the next step the material was homogenized with an APV1000 (SPX, USA) homogenizer (solid content 1%) working in the following way: the suspension is pressed through a narrow pipe having a small gap at its end. This result in high shear forces causing the delamination of the microfibrils from bigger fibers. To prevent the fibers from getting stuck in the homogenizer, the pressure was gradually increased: In the first cycle, fibers were passed through the homogenizer without applying any pressure. In the second cycle a pressure of 100 bar and in the third one a pressure of 400 bar was applied. Homogenizing pressure in the following seven passes was held constant at 800 bar [22].

Microfibrillated cellulose (MFC) was taken as a reference material: it was produced from bleached wheat straw pulp at EMPA (http://www.empa.ch). This MFC was produced using a Masuko Supermass Colloider grinder system.

2.3 Chemical analysis of the material

The lignin content of the different variants of fibrillated material was determined gravimetrically from the dry residue after total acid hydrolysis of carbohydrates.

The first stage of hydrolysis was performed in 72 w% concentrated sulfuric acid (72 w%, Merck, Darmstadt) at 30 °C for 60 minutes The second hydrolysis stage was performed after dilution to 2.6 % acid concentration at 120 °C and 0.12 MPa for 30 minutes. The content of glucose and xylose was determined by means of acid methanolysis followed by gas chromatography for MFC, and by Borat-AEC of sulfuric acid hydrolysates for all other variants, respectively [18], [23]. The results of the analysis are displayed in **table*Table 2*.** The MFC type used for reference was virtually free of lignin and contained only small amount of hemicellulose (< 10%).

Konrad Lorenz Straße 24, A-4330 Tulln an der Donau,
sabine.herzele@boku.ac.at

Table 2: *Chemical composition of the MFLC specimens*

Specimen type	Lignin content [%]	Glucose [%]	Xylose [%]	Mannose [%]
$MFLC_1$	17,0	56,22	16,04	1,31
$MFLC_2$	14	62	14,09	1,41
$MFLC_3$	8,5	80,58	8,73	1,08

2.4 Spray drying

After the homogenization process the fiber suspensions were diluted to a solid content of ~0.5 % and converted into powder by spray drying and a power of 7 kW (ANHYDRO, Denmark). Spray dryers are applied for a long time in the food industry. For example, they allow producing dry dairy products such as milk powder in a large scale. However, one can take advantage of the properties of spray dryed products in other technological areas. For this research project, the fabrication of individual small particles was particularly of interest. In our case, the inlet temperature was 200-220 °C; the outlet temperature was 80 °C. A pressure of 1.5 bar was applied. The dried powder was then collected directly into a plastic bag and sealed under vacuum. This was done to avoid contamination as well as agglomeration of the powder (caused by its hygroscopic character) due to ambient humidity

Preconcentration of the feeding liquid to an appropriate viscosity is a required first step. To high solid concentration leads high viscosity of the suspension resulting in a blockage of the nuzzle of the spray dryer.

In spray drying six general steps are involved. The first step is the preconcentration of the liquid. In the second step atomization is performed. This step consists in splitting the suspension in numerous droplets due to the application of a slight air overpressure combined with a specific nozzle shape. Consequently, the material penetrating in the inside of the spray dryer has a very high surface. In a third step the dehydration in a stream of hot gas is performed. In the fourth step the powder separation takes place. Step number five involves the cooling of the material and number six with the packaging.

The morphology of the particles is mainly determined by the following four steps:

preconcentration of the liquid feed, atomization,hot air drying, and cyclone separation. 5

A major advantage of the spray drying technique is that the product is exposed to a high temperature for a very short range of time only.

3. Instruments and methods

Basically two instruments were used at the Advanced Structures and Composites Center.

The **particle size analyzer G3** (Malvern) can be seen in **figure *Figure 2***.

The second device used was the **inverse gas chromatography** device (IGC) (Surface Measurement

3.1 Particle size analyzer

With the particle size analyzer thousands of individual particles can be characterized within one measurement.

The device allows for quantitative characterization of particle size distribution. Among other parameters like the particle size and shape can be analyzed.

The principal operation mechanism is based on optical microscopy and digital image analysis software.

To ensure uniform and reproducible distribution of the powder on the glass slide, the powder disperser is used.

The optical microscopy images of the three-dimensional particles are captured by a two-dimensional high-resolution camera, identified by using digital thresholding techniques and then analyzed to determine their particle size and shape.

To obtain a 3D image of the particles Z stacking can be used. With this technique several images at different Z heights are taken and the overlaid which results in a 3D image of the particle.

The area of captured 2D image for each particle is converted to a circle of equivalent area. The diameter of the circle is reported as the circle equivalent (CE) diameter of the particle.

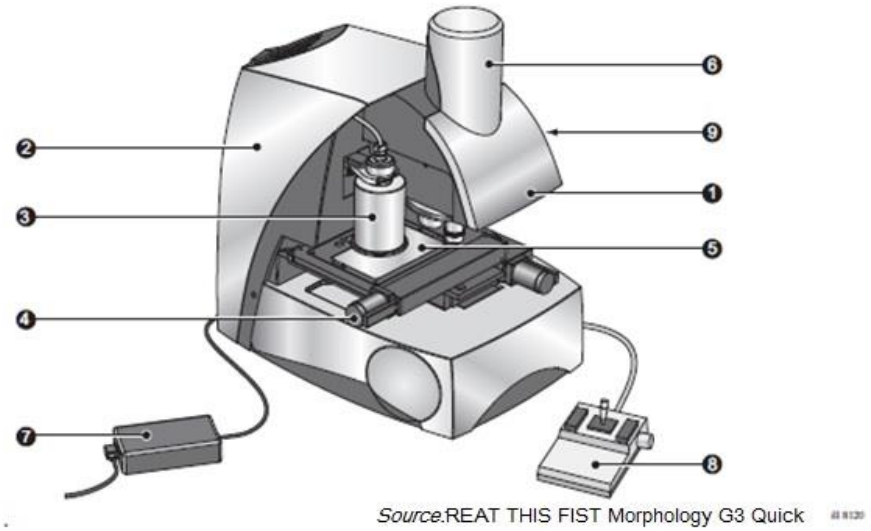

*Source:*REAT THIS FIST Morphology G3 Quick

Figure 2: *Particle size analyzer G3 (Malvern), the component are: 1 optical unit, 2 back panel connections, 3 Integral SDU (G3S only), 4 precision XY stage, 5 sample plate holder and sample plate, 6 FireWire™ digital camera (under removable part of cover), 7 40V power supply for control electronics, 8 Joystick for moving manually*

3.2 Inverse Gas Chromatography

Inverse gas chromatography is a technique to characterize the surface energy γ on the solid surface of granular or fibrous materials. In contrast to analytical gas chromatography, in IGC the column with the material is the stationary phase and the probe gas is the mobile phase.

The principle of IGC relies on the fact that the time needed for well-characterized probe gases to travel through a column filled with a powder of unknown surface chemistry, depends on the type and intensity of surface-chemical interaction between the gas and the powder to be characterized. Thus by carefully choosing the range of probe gases used, comprehensive information on the surface chemistry of the powder can be obtained.

In this study the so-called pulse experiment is conducted to characterize the dispersive surface energy (van der Waals forces) of materials. A defined amount of different probe molecule is one after the other injected and flows with the helium carrier gas through the powder in the column. Since the adsorption isotherm is supposed to be located in the Henry´s low region, the probe molecule is injected at infinite dilution at low vapor pressure.

The lateral interactions among the probe molecules are negligible and the adsorption depends only on adsorbate–adsorbent interactions [24]. At the same time, the number of injected molecules cannot form full monolayer coverage which leads to a primarily interacts with high surface energy sites on the surface. As a consequence mainly information about the highest activity or enthalpy of adsorption on the material surface can be obtained [25].

When the probe molecules exit the column, it is detected by a flame ionization detector (FID).

The actual measured experimental parameter obtained from the measurement is the retention time of the probes molecule.

This can be converted into net specific retention volume by using **equation1**.

$$V_N = \frac{j}{m} \times F \times (t_R - t_0) \times \frac{T}{273{,}15} \qquad (1)$$

$V_N =$ net specific retention volume per gram of sample ($\frac{ml}{g}$)

$T =$ column Temperature (K)

$m =$ weight of sample in column (g)

$t_{R=}$ retention time of the probe (min)

$t_{0=}$ retention time of the reference gas in this case methane (min)

When the net specific retention time for the n-alkane probes is calculated the relationship shown in **equation 2** can be applied.

$$RT \times \ln\left(V_N^{alkane}\right) = 2N \times a \times (\gamma_S^{LW})^{\frac{1}{2}} \times (\gamma_L^{LW})^{\frac{1}{2}} + C \qquad (2)$$

V_N^{alkane}= net specific retention volume of n-alkane probes (ml/g)

γ_L^{LW}=dispersion components of the surface energy of the probe (ml/g))

γ_S^{LW}=dispersion components of the surface energy of the powder surface (ml/g)

N = Avogadro´s number (6.02.10^{23} mol^{-1})

a= surface area of the probe molecule (m²)

C = constant: depending on the reference state of adsorption

R = 8.314 ($\frac{kgm^2}{s^2 mol}$) is the gas constant

T is the absolute temperature (K)

Plotting $RT \times \ln\left(V_N^{alkane}\right)$ against $(\gamma_L^{LW})^{\frac{1}{2}}$ yields a line where the slop equals $2N \times a \times (\gamma_S^{LW})^{\frac{1}{2}}$. From this the disperse component of the surface energy of the powder in the column can be identified. The plot is shown in **figure*Figure 3*.**

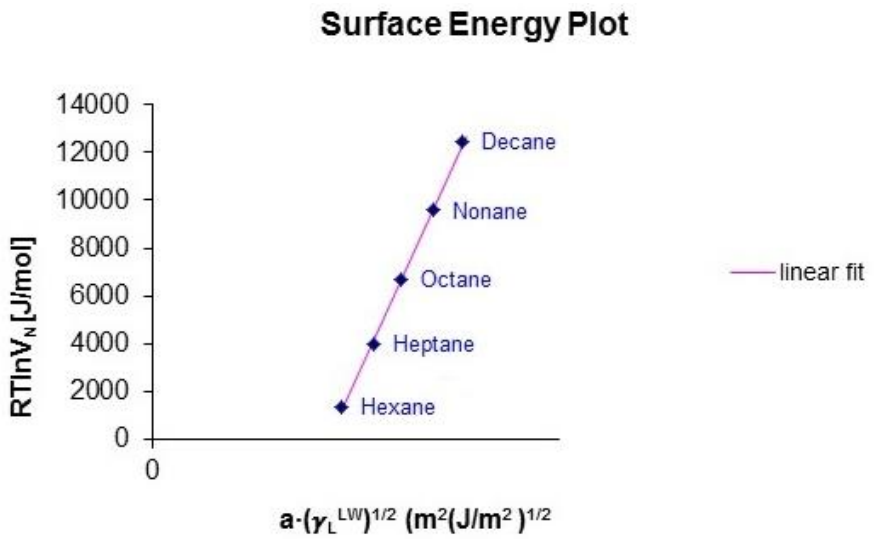

Figure 3: *Schematic calculation of surface energy*

To gain information about the Lewis acid-base properties of the powder surface, polar probes are used. The free energy of adsorption caused by Lewis acid-base interaction is determined by the subtraction of the of the dispersion component from the total free energy. The arithmetic operation is shown in **equation 3** and **4.**

$$-\Delta G_A^{A-B} = -(\Delta G_A^{polar} - \Delta G_A^{ref}) \quad (3)$$

Konrad Lorenz Straße 24, A-4330 Tulln an der Donau,
sabine.herzele@boku.ac.at

$$= -(RT \times \ln(V_N^{polar}) - RT \times (\ln(V_N^{ref})) \quad (4)$$

ΔG_A^{A-B}= free energy of adsorption caused by Lewis acid-base interaction

ΔG_A^{ref}= dispersion component of free energy of adsorption

ΔG_A^{polar} = total free energy of adsorption

$RT \times (\ln(V_N^{ref})$ in equation 4 is the corresponding value of

$RT \times \ln(V_N^{alkane})$ in equation 2 with the molecular descriptor $a \times (\gamma_L^{LW})^{\frac{1}{2}}$ of the polar probe. To obtain ΔG_A^{A-B} the free energy of adsorption, the polar probe is injected at different column temperatures (K).

The Free energy of adsorption is related to the enthalpy of adsorption as shown in **equation 5**.

$$\Delta G^{AB} = \Delta H^{AB} - T\Delta S^{AB} \quad (5)$$

Plotting ΔG_A^{A-B} against column temperatures (K) the intercept is DH^{AB}.

Gutmann's approach of using electron donors and acceptors for the enthalpy of acid–base interactions can finally be applied. The relation is shown in **equation 6**.

$$-\Delta H_A^{A-B} = K_A \times DN + K_B \times AN^* \quad (6)$$

AN* and DN are the acceptor number and donator number of the probes [26] [27]: KA and KD and KB are the acid and base parameters of the adsorbent, which can be determined by plotting $-\Delta H_A^{A-B}$ against $\left(\frac{DN}{AN^*}\right)$. The linear slope and y-intercept are KA and KD, respectively. These numbers are dimensionless and provide comparative information about the material surface under investigation [7].

3.3 Specimen preparation for inverse gas chromatography measurement

The dispersion components of surface energy as well as the acid-base character for all powders were calculated from IGC-measurement at different temperatures.

In the IGC experiments several n-alkane vapor probes were used to determine the dispersive surface free energy of the solid. Polar probes are used to determine the acid-base parameter of the solid. All probe liquids that were used in this study are listed in **table Figure** *3*.

Table 3: *Physical constants for probes used in inverse gas chromatography (IGC) experiment*

Probe	**Surface Tension (γ_L^{LW}, mJ/m^2)**	**Cross Sectional Area (a,m^2)**	**DN[a] (kcal/mol)**	**AN*[b] (kcal/mol)**
n-hexane	18,4	5,2E-19	-	-
n-heptane	20,3	5,7E-19	-	-
n-octane	21,3	6,3E-19	-	-
n-nonane	22.7	6,9E-19	-	-
n-decane	23,4	7,5E-19	-	-
Ethyl acetate	19,6	3.3E-19	17,1	1,5
1,4 dioxane	33,2	3,1E-19	14,8	0
Acetone	16,5	3,4E-19	17,0	2,5
Chloroform	25,0	4.4E-19	0	5,4

Before the specimens were prepared for IGC-measurements all powders were conditioned for 24 hours at 103 °C.

The experiment was run on a SMS-IGC device (Surface Measurement Systems, London, UK). The powders were filled in specific pre-silanized glass columns with dimensions of 30 cm in length and 4 mm in inner diameter. The glass column was sealed with silanized glass wool on one side before the desired amount of powder was filled into the tube. To obtain proper packing of the powder in the tube, it was densified with an electric vibrator. After that the second end of the column was also sealed with glass wool. The packed column is shown in **figureFigure** *4***.**

After mounting the column into the IGC-device, the samples were conditioned for 2 hours at 103 °C at a relative humidity of 0% and a helium carrier gas flow of 10 standard cubic centimeters per minute (sccm). The re-conditioning was performed to avoid moisture effects on the measurement.

In the next step the actual measurement at column temperatures of 40 °C, 50 °C and 60 °C with a relative humidity of 0 %, a helium carrier gas flow of 10 sccm, and a probe vapor concentration of 0.03 p/p0 (p is the partial pressure, p0 is the vapor pressure) was carried out. Methane was used for the reference measurements.

The retention time of the probe gases was detected by a flame ionization detector.

The measurement was carried out in duplicate for each specimen.

Konrad Lorenz Straße 24, A-4330 Tulln an der Donau,
sabine.herzele@boku.ac.at

Figure 4: *IGC column filled with MFLC*

3.4 Specimen preparation for particle size measurement

For all MFC-samples particle size measurements were carried out in duplicate, using a particle size analyzer G3 (Malvern). To achieve reproducible volume amounts of material for each particle size measurement, a 5 mm^3-measuring spoon was used. The specimen holder was sealed on the bottom with a 25 µm thick aluminum foil. Then the spray dried powder was put into the holder. After that, the top of the specimen holder was also sealed with a 25 µm thick aluminum foil. The holder was placed in the powder disperser unit of the particle size analyzer. For uniform distribution on the glass plate the following parameters were used: dispersing air pressure 0.5 MPa, injection time 10 ms, and settling time 60 s. The dispersed powder on the glass plate is shown in **figure Figure** 5.

2D images of the 3D particles were taken by using an objective lens with a 2.468 magnification. To obtain a 3D image of the particles Z stacking with two more layers was used. Images were taken at a Z height of 0, 3,6, and 7,3 lm. The software converts the image of the particles into a circle with an equivalent area. This is called the circle equivalent (CE).

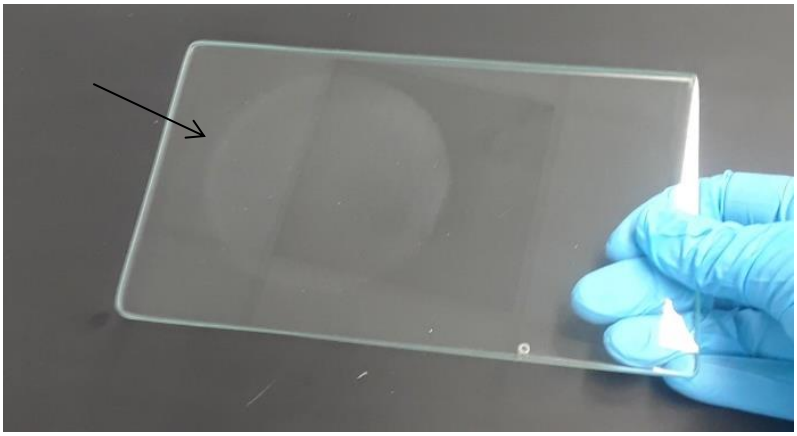

Figure 5: *Specimen on the glass plate of the particle size analyzer*

4. Results and discussion

4.1 Inverse Gas Chromatography

Dispersion component of surface free energy

For all specimens the dispersion component of the surface free energy was determined by using several n-alkanes. To calculate the dispersion component of the surface free energy at least four different alkanes are needed. The alkanes used in this study are listed in **table Table *3***.

The results of the dispersion component of the surface free energy for $MFLC_{1-3}$ at 40 °C, 50 °C and 60 °C are listed in **table Table *4***. For all specimens the dispersion component of the surface free energy decreased by the temperature increase.

Regarding the dispersive component of the surface energy γ_S^d the mijority of reported values fall within the range of 40-50 mJ/m² [28] Within the same temperature range the three MFLC powers with different lignin, cellulose and hemicellulose composition, do not show magnificent differences in their dispersion surface free energy values. At 40 °C the values range between 36,7 and 37,6 mJ/m^2. At 50°C the values range between 33,9 and 35,6 mJ/m^2 and at 60 °C the values are in the range between 33,4 and 35,1 mJ/m^2.

In contrast to these results the reference material of pure cellulose shows significant higher values for the dispersion component of the surface free energy at all three temperatures. At 40 °C the values range between 43,8 ± 1,77 mJ/m². At 50 °C the values range between 41,3 ± 1,2 mJ/m^2 and at 60 °C the values are in the range between 38,3 ± 0,8 mJ/m^2. The dispersion component of the surface free energy γ_s^d of cellulosic material mainly depends on the presence and concentration of free hydroxyl groups on the surface [29]. More hydroxyl groups on the surface are concurrent with higher values of γ_S^d [7]

Since no work of IGC measurements on MFLC powders had been published so far, a comparison to values obtained from literature is not possible.

Comparing the results for MFLC with results from surface modified materials it can be seen, that results after surface modification range in the same region or below the obtained results for MFLC.

Gauthier et.al. [28] reported great decrease in dispersion component of surface free energy due to esterification of cellulose powders by valeryl (C5) and palmitoyl (C16) chlorides. The values for the dispersion component of surface free energy obtained at 70 °C for C5 ranged between 36,2 and 32,1 mJ/m² and for C16 between 28,5 and 28,4 depending on the degree of substitution of hydroxyl groups.

Esterification of cellulose with fatty acids (C11, C18) showed results in the same range [30].

The temperature coefficient of dispersion component of surface energy γ_S^d / mJ/dT is also shown in **Table 4**.

The highest value within the temperature range 40-60° is obtained for MFC (0,28 mJ/(m2 K ±0,06). All MFLC specimens have significantly lower temperature coefficients than MFC.

These findings indicate a higher effect of temperature on the dispersion component of surface energies of MFC than on the MFLC powders.

$MFLC_1$ shows a temperature coefficient of -0,13 mJ/m2K ±0,06, $MFLC_2$ shows a coefficient of -0,16 mJ/m2K ±0,05 and $MFLC_3$ of -0,17 mJ/m2K±0,05.

It should be mentioned, that pre-experiments without preconditioning at 103 °C for 24 hours were performed as well. These results show higher dispersion component of surface free energy and a higher temperature coefficient. The results of this experiment are described and explained in detail in the section:

"6.1 IGC pre-experiment".

Table 4: *Dispersion component of surface energy (γ_s^d) at 40 °C, 50 °C and 60 °C, temperature coefficient of dispersion component of surface energy ($d\gamma_s^d/dT$), acid-base parameter K_A and K_B of the dried MFLC*

Specimen Type	40 °C γ_s^d [mJ/m²]	50 °C γ_s^d [mJ/m²]	60 °C γ_s^d [mJ/m²]	$d\gamma_s^d/dT$ [mJ/dT]	K_A	K_B	K_A/K_B
MFLC1.1	36,7	34,9	34,9	-.0,09	0,19	0,07	2,7
MFLC 1.2	36,8	35,1	33,4	-0,17	0,19	0,17	1,1
MFLC 2.1	37,6	35,6	33,8	- 0,19	0,17	0,7	0,24
MFLC 2.2	37,5	35,2	35,1	-0,12	0,09	0,67	0,13
MFLC 3.1	37,6	35,5	34,1	- 0,18	0,13	0,99	0,13
MFLC 3.2	36,7	33,6	33,4	- 0,17	0,14	0,46	0,30
Ref.MFC1	42,6	40,4	37,7	- 0,25	-	-	-
Ref.MFC2	45,1	42,1	38,8	- 0,32	-	-	-

Acid and base parameters

With IGC measurements using polar probes, the Lewis acid–base characteristics of the MFCL was obtained. The results are shown in **table 4**. The calculation of the acid base parameters for the reference material did not result in reliable parameters. For this reason, they are not shown in **Table 4**.

To characterize the acid base properties of the material, the polar probes ethyl acetate, 1,4 dioxane, acetone and chloroform were used. (**Table 3)**

Based on the theory of Schultz et al. [31], no specific interaction occurs between two acids or two bases.

The acid and base parameters for The MFLC sample were calculated based on the IGC measurements performed at 40, 50 and 60 °C.

Konrad Lorenz Straße 24, A-4330 Tulln an der Donau,
sabine.herzele@boku.ac.at

The acid and base parameters for MFLC specimens have an amphoteric character (acidic and basic). $MFLC_1$ shows a more acidic character while $MFLC_2$ and $_3$ a more basic character is dominant over the acidic one (KB>KA).

This difference in surface chemistry coincides with the fact that differently from MFLC1, MFLC2 and 3 were delignified with the help of small amounts of sulphuric acid added as a catalyst.

4.2 Particle size analysis

Table 5: *Results from particle size measurements for $MFLC_{1-3}$ and MFC*

Specimen	Number of particles	CE Diameter Mean (µm)	HS Circularity Mean	Aspect Ratio Mean
$MFLC_{1.1}$	290810	7,28	0,715	0,658
$MFLC_{1.2}$	157490	6,73	0,740	0,680
$MFLC_{2.1}$	319224	6,10	0,783	0,724
$MFLC_{2.2}$	675510	6,49	0,774	0,717
$MFLC_{3.1}$	619772	5,91	0,832	0,761
$MFLC_{3.2}$	597769	5,89	0,841	0,759
Ref. material 1	128247	7,21	0,848	0,761
Ref. material 2	121985	7,96	0,840	0,764

Particle morphology and particle size distribution are two critical factors in determining properties

of dried powders (wettability, stability, and cohesiveness or dispersability) and their applications in composites. [32-33]

Quantitative characterization of the particle size distributions for thousands of particles was performed by means of the particle size analyzer G3.

The number of particles per measurement, the mean values for the diameter (CE), the circularity (HS) and the aspect ratio for particle size analysis are listed in **Table 5**.

The mean value of the CD for of both measurements within one sample group are: $MFLC_1$ 7,00 µm ± 0,389, $MFLC_2$ 6,30 µm ± 0,28, $MFLC_3$ 5,9 µm ±0,0141 and 7,59 µm ± 0,53 for the ref. material. For HS the following values were obtained: $MFLC_1$ 0,7275 ± 0,02, $MFLC_2$ 0,7785 ± 0,00, $MFLC_3$ 0,8365 ± 0,00 and for MFC 0,844 ± 0,00.

The mean values of the aspect ratio were: $MFLC_1$ 0,669 ± 0,02, $MFLC_2$ 0,7205 ± 0,00, $MFLC_3$ 0,76 ± 0,00 and 0,7625 ± 0,00 for MFC.

This shows that for are all samples the CE the HS and the aspect ratio are in a comparable order of magnitude.

The results from aspect ratio calculation prove a particle like shape of the specimens.

To obtain a better understanding of the particle size distribution, representative frequency curves of the circle equivalent (CE) diameter from $MFLC_{1-3}$ and ref. MFC were extracted. The frequency curves are shown in **Figure 6**.

Fifty percent of the $MFLC_1$, $MFLC_2$ and $MFLC_3$ particles are below 5, 69 µm ± 0, 38,5, 21 µm ± 0,10, and 5,475 µm ± 0,69. 90% of CE diameter for $MFLC_1$, $MFLC_2$ and $MFLC_3$ are below 12,91 µm ± 0,156, 11,145 µm ± 0,79 and 11,58 µm ± 2,03. 10% of the CE diameter for $MFLC_1$, $MFLC_2$ and $MFLC_3$ are below 2, 55 µm ± 0,167, 2,515 µm ± 0,049 and 2,665 µm ± 0,01. These results show that the distribution of the partial size for the MFLC powders is quite similar over the groups. Only MFC shows a slightly narrower frequency curve which is shifted to the right in comparison to the MFLC frequency curves. This means that the smallest particles for MFC are bigger than the for MFLC specimens.

It needs to be taken into account that a particle size under 0,2 µm cannot be recognized with this characterization technique due to the resolution limit of the microscope of the particle size analyzer.

In addition to the quantitative analysis of the specimens also the morphology was studied with atomic force microscopy (AFM) and scanning probe microscopy (SEM).

The findings are described in the "6.2 Topography of specimens" section.

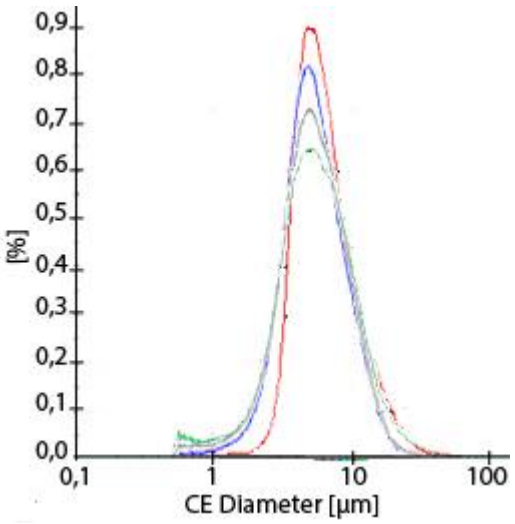

Figure 6: *Particle size distribution of $MFLC_1$ (green), $MFLC_2$ (grey), $MFLC_3$ (blue), MFC (red)*

5. Conclusion

The work performed at the Advanced Structures and Composites Center showed that the surface chemical properties of MFC can be tuned towards reduced hydrophilicity **with high residual lignin- and hemicellulose content of the microfibrillated cellulose.**

A reduction of the dispersion component of surface energy caused by residual lignin and hemicellulose was proven by IGC measurements. This reduction may cause the improved miscibility with non-polar polymers. The results obtained show the same tendency of the reduced of dispersion surface energy like some reported results of surface modified celluloses.

Residual lignin and hemicellulose in MFLC instead of modification of MFC seem to be an interesting path worth following since chemical surface modification is very efficient with regard to establishing compatibility between MFC and hydrophobic polymers, but it adds additional cost to MFC production. The particle size analysis showed that the residual lignin and hemicellulose content in MFLC $_{1\text{-}3}$ in comparison to MFC did not have negative influence on the particle size obtained by spray drying.

The contribution of the lignin, hemicellulose and cellulose composition of MFLC on the dispersion component of the surface free energy could not be explained by IGC measurements. For this reason, further information about the surface chemistry of $MFLC_{1\text{-}3}$ should be obtained. For this x-ray photon spectroscopy (XPS) a surface sensitive technique that gives information about the carbon and oxygen chemistry at the surface of the specimens needs to be performed.

6. Additional results

6.1 IGC pre-experiments

During my stay several challenging situations in the lab occurred.

To give one example I report on the solution for unreliable KA and KB values obtained from IGC measurements in the pre-experiment. Furthermore, this example should point out how a unsuccessful experiment on the first impression can lead to additional information about the characterized material.

After the first run of IGC- experiments was finished, I started to analyze the data. It turned out that the KA and KB values for $MFLC_{1\text{-}3}$ showed no correct results. The results for KA and KB obtained from these measurements are shown in **Table 6**. Some KA and KB values show negative values. Since this should not be the case for this specimens. After consulting my host, Prof. Gardner who asked about my conditioning parameters used in this experiment, the conditioning for the pre- experiment was performed at 30 °C for two hours in the IGC oven.

He told me that the conditioning might have to be performed for a longer time and at higher temperatures due to potential residual volatiles in the specimen that can influence the measurement negatively.

After this discussion the experiment was repeated. This time all specimens were conditioned at 103 °C for 24 hours. Then they were filled into the silanized columns and condition in the oven of the IGC machine at 103 °C for two more hours. After that the actual measurement started. The results obtained from this measurement are already described in detail in the main section of this report. (**Table 4**)

Table 6: *Dispersion component of surface energy (γ_s^d) at 40 °C, 50 °C and 60 °temperature coefficient of dispersion component of surface energy ($d\gamma_s^d/dT$), acid-base parameter K_A and K_B of the dried MFLC*

Specimen type	40 °C γ_s^d [mJ/m²]	50 °C γ_s^d [mJ/m²]	60 °C γ_s^d [mJ/m²]	$d\gamma_s^d$ [mJ/dT]	K_A	K_B
$MFLC_{1.1}$	38,87	34,77	34,18	-0,23	-0,18	0,24
$MFLC_{1.2}$	37,59	35,11	33,84	-0,19	-0,41	0,95
$MFLC_{2.1}$	39,93	35,91	33,15	-0,34	0,54	1,12
$MFLC_{2.2}$	39,57	36,74	33,41	-0,31	0,31	1,93
$MFLC_{3.1}$	38,82	35,97	33,10	-0,29	0,71	-0,34
$MFLC_{3.2}$	38,52	36,65	33,04	-0,27	0,69	-0,06

Comparing the results from the pre-experiment (**Table 6**) and the final experiment (**tTable 4**) it can be seen, that the KA and KB values become positive as desired.

A side effect of the rearrangement of the experimental setup in terms of conditioning time and temperate was, that now also the impact of high temperature (103 °C) over a quite long time (24 hours) on the dispersion component of the surface free energy could be studied.

Comparing the dispersion component of surface energy from the two measurements directly, a clear correlation between conditioning time and temperature increase and a decrease in the dispersion component of the surface free energy can be identified

At 40 °C the values in the final experiment ranged between 36,7 and 37,6 mJ/m^2. At 50 °C the values range between 33,9 and 35,6 mJ/m^2 and at 60 °C the values are in the range between 33,4 and 35,1 mJ/m^2.

These finding consequently also lead to an increase of temperature coefficient in the pre-experiment compared to the final experiment.

In the pre- experiment the following mean values of the temperature coefficient were obtained: $MFLC_1$ -0,21 mJ/m2K ±0,03, $MFLC_2$ -0,32 mJ/m2K ±0,02 and $MFLC_3$ of -0,28 mJ/m2K±0,00.

In contrast to that $MFLC_1$ in the final experiment shows a temperature coefficient of -0,13 mJ/m2K ±0,06, $MFLC_2$ shows a coefficient of -0,16 mJ/m2K ±0,05 and $MFLC_3$ of -0,17 mJ/m2K±0,05.

In the pre-experiment the values for the MFLC powders at 40 °C ranged between 38,5 and 39,9 mJ/m^2. At 50°C the values range between 34,8 and 36,7 mJ/m^2 and at 60 °C the values were in the range between 33 and 34,2 mJ/m^2.

These findings together with the higher dispersion component of the surface energy from the pre-experiment do not only show that the dispersion component of the surface free energy is higher for MFLC without pre-conditioning, it also shows that without pre-conditioning the dispersion component of surface free energy is more sensitive to temperature changes (40 °C-60°C).

From literature it is known that treatment which temperature can lead to surface deactivation [34], [35].

Konrad Lorenz Straße 24, A-4330 Tulln an der Donau,
sabine.herzele@boku.ac.at

As a side effect of the modification of the experimental setup, the combination of the results from the final and the pre-experiment enabled us to show, that IGC-measurement can be a suitable technique to directly study the chemical inactivation of material surfaces caused by temperature.

6.2 Topography of specimens

Atomic force microscopy AFM Images

To document the morphology change of the specimens caused by the spray drying process, atomic force microscopy measurements (AFM) were performed before the spray drying and scanning probe microscopy images (images) were conducted after the drying process. This is justified by the fact that no difference could be observed among the samples when using optical microscopy. Atomic force microscopy allows going to the nanometer level and assessing potential differences in the fibrillated structure.

AFM-topography measurements for all fibril suspensions before spray drying were performed with a Dimension Icon AFM (Bruker AXS, France; formerly Veeco). The samples for the measurement were prepared by depositing a drop of fibril suspension on a mica plate and subsequent evaporation of water at ambient conditions was investigated. The fibril-water suspension had a content of 0.001% which allows for single fibril characterization.

All scans were performed using Bruker's ScanAsyst-Air probes (k = 0.4 N/m, f0 = 70 Hz, r = 2 nm; nominal values, probe-specific data calibrated before scans). Scanning rate was set to 2,5 µm/s for all measurements. Tip frequency was set to 1 kHz and peak-force set point to 6 nN. Output data was evaluated using Gwyddion Image Analysis (V2.39) freeware.

The topography images obtained For MFC1-3 shown in **Figure 7** do not show distinct differences in the degree of fibrillation. The topography images show a high degree of fibrillation ranging from tenths of nm to several hundred nm. Comparing these results to the reference material it clearly can be seen that MFLC can be fibrillated to a comparable fineness as is observed regularly for MFC produced from bleached, essentially lignin-free pulp.

Konrad Lorenz Straße 24, A-4330 Tulln an der Donau,
sabine.herzele@boku.ac.at

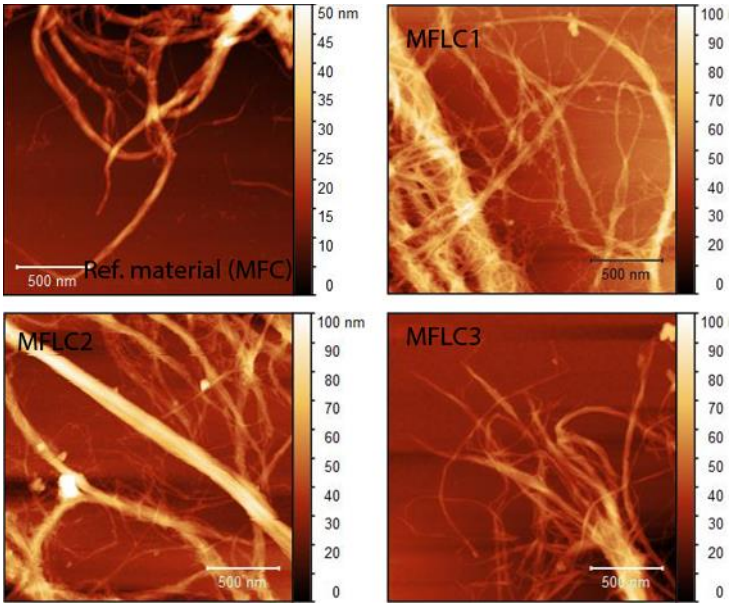

Figure 7: *Atomic force microscopy (AFM) topography images of MFLC$_{1-3}$ and MFC*

Scanning probe microscopy (SEM) images

The specimens were placed on aluminum specimen holders, sputter coated with a platinum layer of about 7.5 nm (BAL-TEC MED 020 Modular High Vacuum Coating Systems, BAL-TEC AG, Liechtenstein) using Ar as a carrier gas at 0.05 mbar and SEM was carried out using a FEI Nova NanoSEM 230 instrument (FEI, Hilsboro, Oregon, USA) at an accelerating voltage of 20 kV and a working distance of 5 mm.

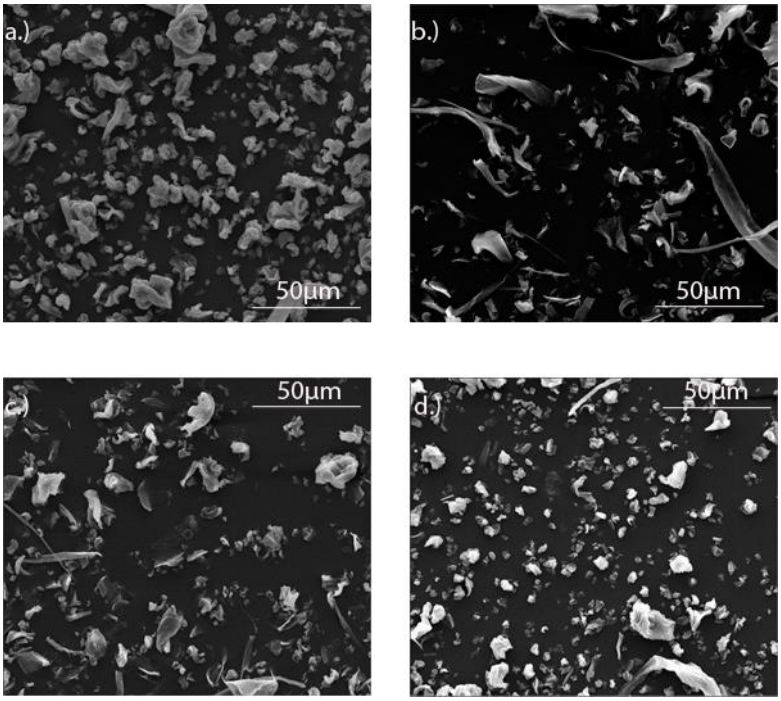

Konrad Lorenz Straße 24, A-4330 Tulln an der Donau,
sabine.herzele@boku.ac.at

Figure 8: *Scanning probe microscopy images (SEM) of spray dried a.) Ref. material (MFC), b.) $MFLC_1$, c.) $MFLC_2$ and d.) $MFLC_3$*

The SEM images for all specimens after the spray drying are shown in **Figure 8.** Individual particles of variable sizes with a rather particular than fibrillary geometry can be seen. This heterogeneity in particle size within one sample group is well in line with the finding from the particle size measurements. It is a well-known fact that during the spray drying processes, the fibrils, shown in **Figure 7** pack together to particle and form agglomerates.

Konrad Lorenz Straße 24, A-4330 Tulln an der Donau,
sabine.herzele@boku.ac.at

7 References

1.Gardner, D. J.; Oporto, G. S.; Mills, R.; Samir, M. A. S. A., Adhesion and surface issues in cellulose and nanocellulose. *Journal of Adhesion Science and Technology* **2008,** *22* (5-6), 545-567.

2.Hubbe, M. A.; Gardner, D. J.; Shen, W., Contact angles and wettability of cellulosic surfaces: A review of proposed mechanisms and test strategies. *BioResources* **2015,** *10* (4), 8657-8749.

3.Tze, W. T.; Gardner, D. J.; Tripp, C. P.; O'Neill, S. C., Cellulose fiber/polymer adhesion: effects of fiber/matrix interfacial chemistry on the micromechanics of the interphase. *Journal of adhesion science and technology* **2006,** *20* (15), 1649-1668.

4.Peng, Y.; Gardner, D. J.; Han, Y., Drying cellulose nanofibrils: in search of a suitable method. *Cellulose* **2012,** *19* (1), 91-102.

5.Peng, Y.; Han, Y.; Gardner, D. J., Spray-drying cellulose nanofibrils: effect of drying process parameters on particle morphology and size distribution. *Wood and Fiber Science* **2012,** *44* (4), 448-461.

6.Peng, Y.; Gardner, D. J.; Han, Y.; Kiziltas, A.; Cai, Z.; Tshabalala, M. A., Influence of drying method on the material properties of nanocellulose I: thermostability and crystallinity. *Cellulose* **2013,** *20* (5), 2379-2392.

7.Peng, Y.; Gardner, D. J.; Han, Y.; Cai, Z.; Tshabalala, M. A., Influence of drying method on the surface energy of cellulose nanofibrils determined by inverse gas chromatography. *Journal of colloid and interface science* **2013,** *405*, 85-95.

8.Klemm, D.; Kramer, F.; Moritz, S.; Lindström, T.; Ankerfors, M.; Gray, D.; Dorris, A., Nanocelluloses: A new family of nature-based materials. *Angewandte Chemie International Edition* **2011,** *50* (24), 5438-5466.

9.Dufresne, A., Nanocellulose: a new ageless bionanomaterial. *Materials Today* **2013,** *16* (6), 220-227.

10.Mazeau, K., On the external morphology of native cellulose microfibrils. *Carbohydrate polymers* **2011,** *84* (1), 524-532.

11.Habibi, Y., Key advances in the chemical modification of nanocelluloses. *Chemical Society Reviews* **2014,** *43* (5), 1519-1542.

12.Eyholzer, C.; Tingaut, P.; Zimmermann, T.; Oksman, K., Dispersion and reinforcing potential of carboxymethylated nanofibrillated cellulose powders modified with 1-hexanol in extruded poly (lactic acid)(PLA) composites. *Journal of Polymers and the Environment* **2012,** *20* (4), 1052-1062.

13.Jiang, F.; Hsieh, Y.-L., Holocellulose nanocrystals: amphiphilicity, oil/water emulsion, and self-assembly. *Biomacromolecules* **2015,** *16* (4), 1433-1441.

14.Gu, J.; Hsieh, Y.-L., Surface and structure characteristics, self-assembling, and solvent compatibility of holocellulose nanofibrils. *ACS applied materials & interfaces* **2015,** *7* (7), 4192-4201.

15.Wang, X.; Sun, H.; Bai, H.; Zhang, L.-p., Thermal, mechanical, and degradation properties of nanocomposites prepared using lignin-cellulose nanofibers and poly (lactic acid). *BioResources* **2014,** *9* (2), 3211-3224.

16.Ballner, D.; Herzele, S.; Keckes, J.; Edler, M.; Griesser, T.; Saake, B.; Liebner, F.; Potthast, A.; Paulik, C.; Gindl-Altmutter, W., Lignocellulose nanofiber-reinforced polystyrene produced from composite microspheres obtained in suspension polymerization shows superior mechanical performance. *ACS applied materials & interfaces* **2016,** *8* (21), 13520-13525.

17.Yan, Y.; Herzele, S.; Mahendran, A. R.; Edler, M.; Griesser, T.; Saake, B.; Li, J.; Gindl-Altmutter, W., Microfibrillated Lignocellulose Enables the Suspension-Polymerisation of Unsaturated Polyester Resin for Novel Composite Applications. *Polymers* **2016,** *8* (7), 255.

18.Winter, A.; Andorfer, L.; Herzele, S.; Zimmermann, T.; Saake, B.; Edler, M.; Griesser, T.; Konnerth, J.; Gindl-Altmutter, W., Reduced polarity and improved dispersion of microfibrillated cellulose in poly (lactic-acid) provided by residual lignin and hemicellulose. *Journal of Materials Science* **2017,** *52* (1), 60-72.

19.Herzele, S.; Veigel, S.; Liebner, F.; Zimmermann, T.; Gindl-Altmutter, W., Reinforcement of polycaprolactone with microfibrillated lignocellulose. *Industrial Crops and Products* **2016,** *93*, 302-308.

20.Puls, J.; Schreiber, A.; Saake, B., Conversion of beech wood into platform chemicals after organosolv treatment. *Proceedings of the 15th ISWFPC, Oslo, Norway* **2009**.

21.Muurinen, E., Organosolv pulping--A review and distillation study related to peroxyacid pulping. **2000**.

22.Colson, J.; Bauer, W.; Mayr, M.; Fischer, W.; Gindl-Altmutter, W., Morphology and rheology of cellulose nanofibrils derived from mixtures of pulp fibres and papermaking fines. *Cellulose* **2016,** *23* (4), 2439-2448.

23.Willför, S.; Pranovich, A.; Tamminen, T.; Puls, J.; Laine, C.; Suurnäkki, A.; Saake, B.; Uotila, K.; Simolin, H.; Hemming, J., Carbohydrate analysis of plant materials with uronic acid-containing polysaccharides–A comparison between different hydrolysis and subsequent chromatographic analytical techniques. *Industrial Crops and Products* **2009,** *29* (2), 571-580.

24.Dorris, G. M.; Gray, D. G., Adsorption of n-alkanes at zero surface coverage on cellulose paper and wood fibers. *Journal of Colloid and Interface Science* **1980,** *77* (2), 353-362.

25.Balard, H.; Maafa, D.; Santini, A.; Donnet, J., Study by inverse gas chromatography of the surface properties of milled graphites. *Journal of Chromatography A* **2008,** *1198*, 173-180.

26.Gutmann, V., *donor-acceptor approach to molecular interactions*. Plenum Press: **1978**.

27.Fowkes, F. M., Quantitative characterization of the acid-base properties of solvents, polymers, and inorganic surfaces. *Journal of adhesion science and technology* **1990,** *4* (1), 669-691.

28.Gamelas, J. A., The surface properties of cellulose and lignocellulosic materials assessed by inverse gas chromatography: A review. *Cellulose* **2013,** *20* (6), 2675-2693.

29.Garnier, G.; Glasser, W. G., Measuring the surface energies of spherical cellulose beads by inverse gas chromatography. *Polymer Engineering & Science* **1996,** *36* (6), 885-894.

30.Jandura, P.; Riedl, B.; Kokta, B. V., Inverse gas chromatography study on partially esterified paper fiber. *Journal of Chromatography A* **2002,** *969* (1), 301-311.

31.Schultz, J.; Lavielle, L.; Martin, C., Propriétés de surface des fibres de carbone déterminées par chromatographie gazeuse inverse. *Journal de chimie physique* **1987,** *84*, 231-237.

32.Vehring, R., Pharmaceutical particle engineering via spray drying. *Pharmaceutical research* **2008,** *25* (5), 999-1022.

33.Móczó, J.; Pukánszky, B., Polymer micro and nanocomposites: structure, interactions, properties. *Journal of Industrial and Engineering Chemistry* **2008,** *14* (5), 535-563.

34.Gardner, D.; Tze, W.; Shi, S., Surface energy characterization of wood particles by contact angle analysis and inverse gas chromatography. *Advances in Lignocellulosics Characterization. TAPPI Press* **1999,** *12*, 263-293.

35.Koch, P., Utilization of Hardwoods Growing on Southern Pine Sites–Volume 2. *Agricultural Handbook SFES-AH-605. Asheville, NC: USDA-Forest Service, Southern Forest Experiment Station. 1419-2542.* **1985,** *605*, 1419-2542.

Konrad Lorenz Straße 24, A-4330 Tulln an der Donau,
sabine.herzele@boku.ac.at